PCCP

RSC Publishing

PAPER

View Article Online
View Journal | View Issue

Cite this: *Phys. Chem. Chem. Phys.*, 2013, **15**, 2421

Two-dimensional Si_xGe_{1-x} films with variable composition made *via* multilayer colloidal template-guided ionic liquid electrodeposition†

Wuhong Xin,[a] Jiupeng Zhao,[b] Dengteng Ge,[a] Yanbo Ding,[b] Yao Li*[a] and Frank Endres*[c]

Received 8th November 2012,
Accepted 4th December 2012

DOI: 10.1039/c2cp43983b

www.rsc.org/pccp

The binary alloy system Si_xGe_{1-x} provides a continuous series of materials with gradually varying properties. In this paper, we report on a fundamental basis a method to make large-area macroporous Si_xGe_{1-x} films with variable Ge content by electrodeposition in an ionic liquid, with $SiCl_4$ and $GeCl_4$ as precursors. The chemical composition of the products can be modified by changing the molar ratio of the precursors. Periodical macroporous Si_xGe_{1-x} was made by a multilayer polystyrene (PS) template assembled as face-centered cubic lattice. Two-dimensional (2-D) Si_xGe_{1-x} bowl-like and fishing-net structures can be obtained by applying different deposition temperatures. The results highlight the potential applications, including photonic bandgap and battery materials, as well as ultra-thin gratings, due to the effect of modification of light and improved tunability of composition, although Si_xGe_{1-x} made by our method is sensitive to oxidation by air.

Introduction

Two-dimensional (2-D) architectures are, for example, materials with an ordered arrangement of pores with a high specific surface area.[1–9] Such porous arrays are of interest, for example, for the design of catalysts and sensors.[1,2,10]

In general, highly ordered porous materials are often made by colloidal crystal templates assembled into a face-centered cubic (FCC) structure. By a simple two-step replication process, the materials of interest are introduced into the template (*e.g.* by electrochemical means) and the sub-micrometer colloidal spheres are subsequently removed, leaving voids of a given size in the host material. For the fabrication of 2-D materials, a planar microfabrication technique based on a 2-D ordered colloidal monolayer is used in templating the materials. Self-assembly of microspheres and spin-coating techniques are usually used for the fabrication of large 2-D colloidal crystals. However, special equipment is needed in the two techniques and the obtained products normally have numerous defects (*e.g.* vacancies, dislocations because of the fast growth rate of the template). Jiang and coworkers reported a different method using 3-D colloidal crystals as templates to produce 2-D ordered structures.[8]

3-D colloidal templates seem to be an ideal alternative for a good quality of the colloidal crystals and for a simpler synthesis process. However, if physical vapor deposition (PVD) is employed, mainly incompletely filled structures were obtained with many defects.[8] For applications like catalysis, sensors and gratings, an ordered porous and open structure is necessary, allowing direct contact with the underlying surface. The present paper is focused on the fabrication of open structures. The feasibility to grow 2-D ordered structures by atomic layer deposition and electrochemical deposition inside a 3-D template has been shown in literature.[1–9] Compared to atomic layer deposition, electrochemical deposition is a convenient, rapid and cost-effective method (in contrast to X-ray or electron beam lithographic techniques) and is particularly suitable for the deposition of thin supported films in quite a short time.

Usually, ionic liquids have wide electrochemical windows which allow the deposition of semiconductors (such as Si and Ge) that can not be obtained in aqueous solutions.[11] Si_xGe_{1-x} has attracted quite considerable attention, *e.g.* for band structure engineering, photovoltaics and microelectronics.[12–14]

[a] *Center for Composite Materials and Structure, Harbin Institute of Technology, Harbin 150001, China. E-mail: yaoli@hit.edu.cn; Fax: +86-451-86403767; Tel: +86-451-86403767*

[b] *School of Chemical Engineering and Technology, Harbin Institute of Technology, Harbin 150001, China*

[c] *Clausthal University of Technology, Institute of Electrochemistry, D-38678 Clausthal-Zellerfeld, Germany. E-mail: frank.endres@tu-clausthal.de; Fax: +49 (0)5323 72-2460; Tel: +49 (0)5323 72-3141*

† Electronic supplementary information (ESI) available. See DOI: 10.1039/c2cp43983b

In the case of 2-D Si_xGe_{1-x}, the position of the photonic bandgap is determined by the refractive index of the pore wall and the diameter of the pores. Si and Ge are two important semiconductors with high refractive indices of 3.53 at 1.1 μm and 4.12 at 2 μm, respectively. The refractive index of Si_xGe_{1-x} can be changed by altering its composition: a high Ge content gives rise to a higher refractive index, leading to a red shift of the bandgap and vice versa. However, alternatives to obtain tunable Ge content in a wider range are still challenges.

In this paper, we have on a fundamental basis successfully made 2-D ordered Si_xGe_{1-x} with tunable Ge content by multilayer polystyrene (PS) template-assisted electrodeposition at a temperature of 90 °C. The composition can be easily adjusted by variation of the relative $SiCl_4/GeCl_4$ ratio in the ionic liquid. The process is, from the electrochemical point of view, simple and the product has uniform periodical pores and the lateral dimensions of the material are only limited by the electrochemical cell. Interestingly, at a deposition temperature of 90 °C, the formation of 2-D ordered architecture is observed while the deposition carried out at room temperature leads to the formation of a 3-D product as described in ref. 15.

Experimental

Materials

The ionic liquid 1-ethyl-3-methylimidazolium bis(trifluoromethylsulfonyl) amide ([EMIm]Tf_2N, 99%) was purchased from IOLITEC (Germany) in high quality and used after drying under vacuum at 100 °C to a water content of below 3 ppm. $SiCl_4$ (99.998%) and $GeCl_4$ (99.9999%) were purchased from Alfa Aesar and used without any further purification. An equimolar amount (0.1 mol L^{-1}) of $SiCl_4$ and $GeCl_4$ liquid was added to the [EMIm]Tf_2N. The electrolyte was stirred before use to ensure a uniform concentration. The preparation of the electrolyte and all electrochemical experiments were carried out in a glovebox (Vigor Glove Box from Suzhou, China, argon filled) with water and oxygen contents of below 1 ppm.

Monodisperse PS colloidal spheres with an average diameter of 500 nm were obtained using an emulsifier-free emulsion polymerization technique.[16] An alcoholic suspension of monodisperse polystyrene spheres was prepared, then the ITO substrates (1.5 × 2 cm^2) were coated with several layers by a simple dipping process.[17] Within a few seconds this method delivered up to 20 sphere layers. This method is best suited for 3-DOM materials. The PS-coated ITO substrate was used as a working electrode (WE). An Ag wire and a Pt ring were used as quasi-reference electrode (RE) and counter electrode (CE), respectively. The Ag wire gives a more stable reference electrode potential during the deposition than a Pt wire would give.

Fabrication of the 2-D ordered thin films

All the electrochemical experiments were carried out in a argon-filled glovebox. The electrochemical cell and the O-ring in contact with the electrolyte were made of polytetrafluoroethylene (Teflon) and Viton, respectively. The electrochemical cell was clamped over an O-ring onto the PS template on the ITO substrate. After addition of the electrolyte, a constant electrode potential was applied. In the case of electrodeposition at high temperature, the cell was put on a heater at a temperature of 90 °C for 3–5 min before the electrodeposition is carried out to ensure that the electrolyte has been heated to the elevated temperature. The electrolyte was removed from the cell under potential control to reduce a chemical attack of $GeCl_4$ to the deposit as much as possible. The deposit was subsequently removed from the glovebox and rinsed quickly in isopropanol to remove residual $SiCl_4/GeCl_4$/[EMIm]Tf_2N. Finally, the PS template was removed by dimethylformamide (DMF) to get the electrodeposited replica of the PS spheres.

Characterization

All electrochemical measurements were carried out on an electrochemical workstation (CHI 660C, Shanghai Chenhua Device Company, China). The morphology of the deposit was investigated by a high-resolution scanning electron microscope operated at 20 kV (HR-SEM, S-4800, Hitachi) equipped with energy-dispersive X-ray spectroscopy (EDX). The X-ray photoelectron spectroscopic (XPS) analysis of the samples was carried out on a PHI 5700 XPS system. All the binding energies were referenced to the C1s peak at 284.6 eV of surface-contamination carbon. The optical spectra of the templates and of the replicas were obtained using a fiber spectrometer (Maya 2000 Pro, Ocean Optics). Unfortunately, *ex situ* characterization and handling leads to an unavoidable attack of oxygen on the samples with the results of a partial oxidation of the amorphous semiconductor. This problem will be overcome in future by doing the optical characterization inside a glove box and/or by annealing the samples under ultrahigh vacuum before an *ex situ* analysis.

Results and discussion

Electrochemical measurement

Fig. 1 shows the cyclic voltammograms of $GeCl_4$ (black) and of $SiCl_4/GeCl_4$ (red) in [EMIm]Tf_2N on ITO, covered with a 500-nm-diameter PS template of ~20 layers. There are

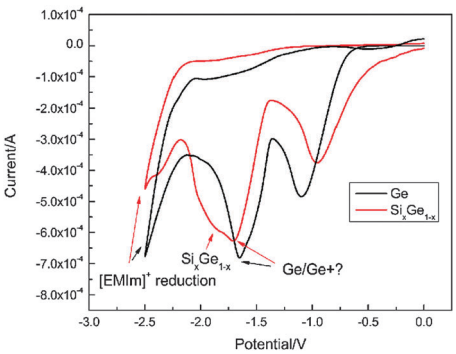

Fig. 1 Cyclic voltammograms of $GeCl_4$ (black) and of $SiCl_4$ + $GeCl_4$ (1 : 1 molar ratio, red) in [EMIm]Tf_2N on ITO, acquired at a scan rate of 10 mV s^{-1} at a temperature of 90 °C.

two main reduction peaks of germanium at potentials of −1.0 V and −1.7 V, corresponding to the reduction of Ge(IV) to Ge(II) and of Ge(II) to Ge(0). A more negative process at −2.3 V is correlated with the decomposition of the $[EIMm]^+$ ion. The red curve reveals that the first peak at −0.8 V corresponds to the Ge(IV) to Ge(II) reduction if $SiCl_4$ is present.[11] The slight shift of the peak position in comparison to the black curve might be due to a different structure of the ionic liquid/electrode interface. The second process at about −1.7 V consists of two reduction processes as discussed in ref. 11: the first process at a slightly higher potential (−1.7 V) is correlated with the reduction of Ge(II) to Ge(0) and some underpotential deposition of silicon, while the second reduction wave at around −1.9 V is related to the complex co-deposition of Si_xGe_{1-x} accompanied with the formation of a brownish-yellow deposit on the polystyrene-covered substrate, which can be easily recognized by the naked eye.

Composition analysis

In order to obtain information on the chemical composition, an XPS analysis was performed on the as-deposited sample obtained at 90 °C. According to the survey spectrum of the deposit surface, the sample contains Si, Ge, O, C and F. The existence of element F is caused by the electrolyte adsorbed on the deposit.[18] Carbon and oxygen can be attributed to some residue of the ionic liquid and to some surface contamination (surface oxidation of the product under *ex situ* conditions).

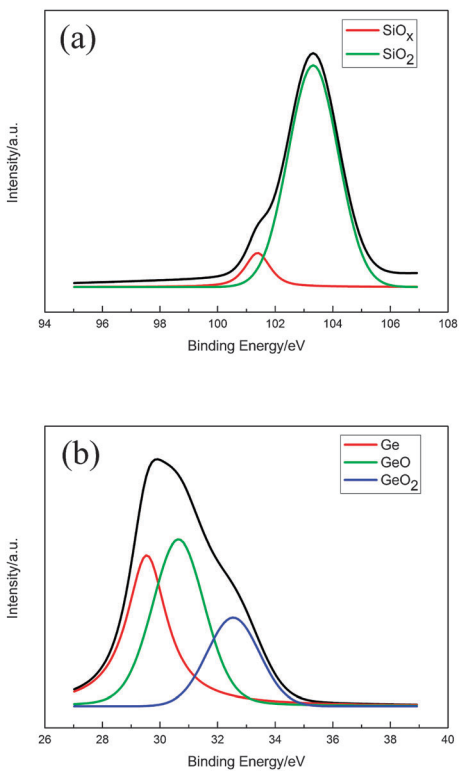

Fig. 2 The Si2p (a) and Ge3d (b) spectra with fitted components on the surface of the product. Si is fully oxidized, Ge only at the surface.

The best fit of Si 2p XPS spectrum (Fig. 2a) was achieved locating peaks at 101.2 and 103.3 eV,[19] which can be correlated with the coexistence of Si^{x+} and Si^{4+} species, demonstrating that the deposited silicon at 90 °C has been oxidized to SiO_x or SiO_2 under air. This is an unfortunate consequence of the reactivity of amorphous silicon. The Ge 3d spectrum of the surface analysis (Fig. 2b) can be resolved into three main peaks at about 29.1 eV, 30.7 eV and 32.2 eV binding energies for monovalent, divalent and tetravalent germanium, indicating that germanium is partially oxidized, too,[20] and the XPS data from the surface analysis also gave the ratio of Ge to Si as 3 to 1. However, such profiles can only give information on the composition of the surface. Preliminary XRD results suggest that Si_xGe_{1-x} is amorphous even if handled under inert gas, but more experiments will be required. In order to determine the ratio of Ge to Si, an additional EDX analysis was performed.

The influence of the concentration ratio of $SiCl_4$ and $GeCl_4$ on the composition of the deposit was studied by adjusting molar ratios of $SiCl_4/GeCl_4$ at 4 : 1, 2 : 1, 1 : 1, 1 : 2 and 1 : 4. An EDX analysis was carried out to study the composition of the deposits after applying a constant potential for 30 min at the potential of −1.9 V. In order to obtain reliable data, all deposition experiments were carried out using Cu substrates as a reference to avoid a falsification by Si from the ITO base material.

The EDX analysis (see ESI,† Fig. S1) shows that the deposits contain Si, Ge, C and O, which is consistent with the XPS result. The composition of the deposits is slightly different from the molar ratio in the ionic liquid (see Table 1). The ratio depends on the diffusion coefficients of $SiCl_4$ and $GeCl_4$ in the liquid and on the applied electrode potential. For simplicity, the deposition described here was done at a constant electrode potential of −1.9 V *vs.* the quasi-reference electrode. A detailed analysis of the composition as a function of the electrode potential will require further fundamental studies as the interfacial layers of ionic liquids might have an influence, too. Nevertheless, the results show that the composition of Si_xGe_{1-x} can be modified by simply changing the molar ratio of $SiCl_4$ and $GeCl_4$ in the solution.

Optical properties further confirmed that the products have unfortunately been partially oxidized under *ex situ* handling. For an opal structure the positions of reflection peaks in the spectra are highly sensitive to the effective refractive index, giving rise to information about chemical composition of the infiltrated materials. The spectra of the inverse opals measured

Table 1 Composition of the electrolytes and of the electrodeposited Si_xGe_{1-x} films

Molar ratio of Si to Ge (electrolytes)	Molar ratio of Si to Ge (deposits)
4 : 1	3.44 : 1
2 : 1	1.44 : 1
1 : 1	1 : 1.04
1 : 2	1 : 2.32
1 : 4	1 : 4.35

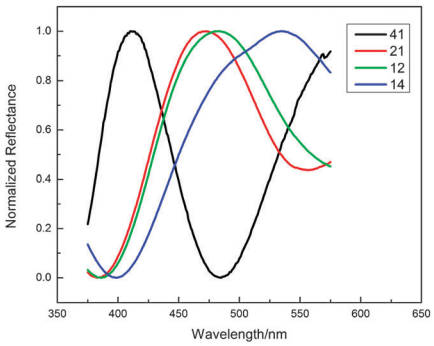

Fig. 3 Vertical reflection spectra of partially oxidized Si_xGe_{1-x} prepared from electrolytes with different molar ratios of $SiCl_4$ and $GeCl_4$. Si : Ge = 4 : 1 (black), Si : Ge = 2 : 1 (red), Si : Ge = 1 : 2 (green) and Si : Ge = 1 : 4 (blue).

have the feature of the Bragg diffraction in the (111) plane which can be expressed by (eqn (1))[21]

$$m\lambda = 2d\sqrt{n_{\text{eff}}^2 - \sin^2\theta} \quad (1)$$

where m is an integer (the diffraction order of the reflection), λ is the wavelength of the diffraction peak, d is the interplanar distance in the [111] direction and θ is the incident angle of the light. n_{eff} designates an effective refractive index of the sample, which can be estimated by (eqn (2))

$$n_{\text{eff}}^2 = f_1 n_1^2 + (1 - f_1) n_2^2 \quad (2)$$

Here, n_1 and n_2 are the refractive indices of air and the materials, and f_1 is the filling volume fraction of air. Fig. 3 shows the reflection spectra (375 nm $< \lambda <$ 575 nm) of the 2-D ordered Si_xGe_{1-x} film prepared by adjusting molar ratios of $SiCl_4/GeCl_4$ at 4 : 1, 2 : 1, 1 : 2 and 1 : 4 through a PS template assembled from 500-nm-diameter spheres. The incident and exitance angles for the experiment were 90°. It can be concluded from the figure that the refraction index increases with the increase of the $GeCl_4$ content in the electrolyte. But the trend is not straightforward, which is presumably due to the oxidation of the products under air – still a shortcoming of electrochemically made Si containing semiconductors. But the results are in agreement with the XPS analysis. At this point we have to say clearly that electrochemically made amorphous Ge is quite robust against an attack by environmental oxygen. Electrochemically made amorphous Si is in contrast quite reactive and transforms within a few minutes to SiO_2 under air. As mentioned above, the problem can be overcome in future by doing the optical characterization inside the glove box and/or by annealing of the material under UHV conditions.

Morphological characterization

The formation of the 2-D ordered products is guided by the polystyrene sphere layer closest to the electrode surface, and the ordering of the top layer can reflect the quality of the bottom layer to some extent. Fig. 4a shows a typical SEM image of a PS template assembled from 500 nm diameter PS spheres on an ITO substrate. The top layer of the colloidal template shows a close-packed hexagonal array with a long-range ordering.

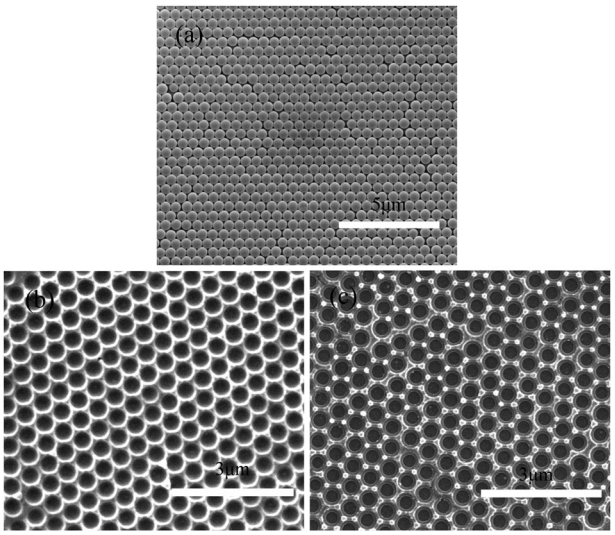

Fig. 4 SEM image of colloidal template assembled from 500 nm diameter PS spheres on ITO substrate (a). SEM images of 2-D thin films electrodeposited at room temperature (b) and at 90 °C (c).

A highly ordered 2-D Si_xGe_{1-x} is made by applying a potential of −1.9 V *vs.* the quasi-reference electrode for 15 min at room temperature and at 90 °C, respectively. The obtained Si_xGe_{1-x} films with a uniform thickness are shown in Fig. 4b and c. The thin films left after removal of PS matrix with DMF well retain the ordered, close-packed structure. The center-to-center distance measured is the same diameter as the one of the colloidal spheres used, confirming that no shrinkage occurred along the (111) direction during the electrodeposition. It is observed that the bottom of the deposit made at room temperature shown in Fig. 4b is different from the one made at 90 °C as shown in Fig. 4c. Compared to the usual bowl-like architecture (Fig. 4b), the ordered architecture presented in Fig. 4c looks more like a fishing-net.

The slightly different structure is explained in the illustration presented in Fig. 5. The elevated temperature applied to the electrochemical cell is considered to be the main reason for the formation of the 2-D ordered Si_xGe_{1-x} with flat bottoms of the bowls. The formation of the point deposits can be understood qualitatively: the colloidal spheres soften and the contact surface between the spheres and the substrate increases when an elevated temperature is applied to the system, as indicated by Fig. 5b. The face-centered cubic symmetry of the sample is partially lost, and the electrodeposition perfectly replicates the templates which are under some uniaxial compression along the sedimentation direction (111). It can be concluded from the illustration that the depth of the bowls made at higher temperature is lower than that one obtained at room temperature. The ''mouths'' of the pores shown in Fig. 5i retain the shape of the original interstitial spaces, but those ones shown in Fig. 5j are rather points than triangular deposits (as indicated by arrows). When the polymer spheres are heated, connections are formed between adjacent

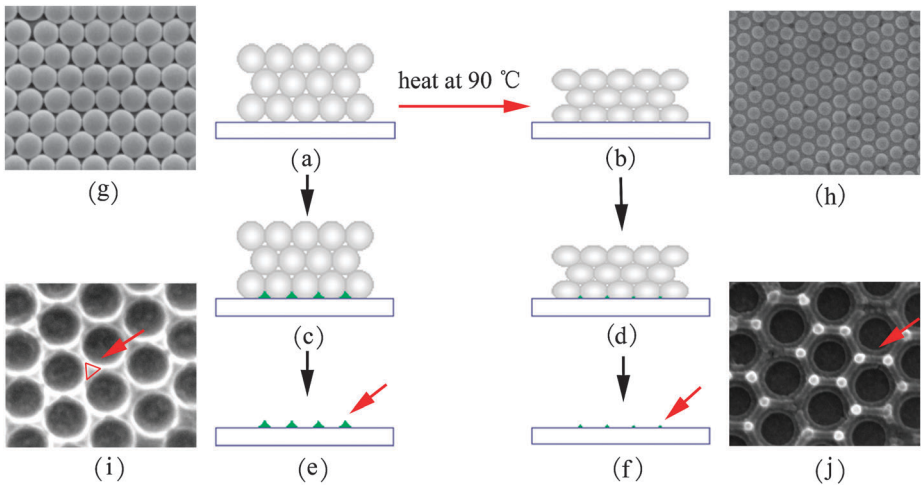

Fig. 5 Illustration of the formation mechanism for the two kinds of 2-D architectures: (a) PS template made by self-assembly; (b) PS template obtained after annealing at elevated temperature; (c) and (d) infiltration of the template by electrodeposition for 15 min; (e) and (f) removal of the PS spheres by DMF to obtain a 2-D films.

spheres, leading to a shrinkage of the interstitial spaces. The shrunk interstices provide fewer spaces for the liquid and the deposit, which limits the formation of the second layer of the inverse opal. Furthermore, the semiconductor precursors are evaporated at this temperature due to the low boiling points of 57.6 and 83.1 °C for $SiCl_4$ and $GeCl_4$, respectively. Therefore, the thickness of the deposit (the depth of the bowl) is limited as the precursors are simply removed from the solution.

Fig. 6 shows SEM images of 2-D ordered architectures prepared at 90 °C over large areas. As indicated by Fig. 5a, the domain size of the template is well retained by the replica over an area of more than 6×10^4 μm^2. The large cracks along the (111) direction of the original template, which can not be avoided during the drying process, can also be seen.[22] Normally, the cracks of the template are filled with the targeted materials with a thickness higher than the ordered architectures, leading to a rough surface of the deposits.[23] Furthermore, other materials like Cu, for example, are left, the cracks remaining unfilled and forming isolated domains.[24] In our experiment, as indicated by the high resolution image Fig. 5b, the original cracks have been filled with Si_xGe_{1-x}. This might be due to the rather slow growth of the deposit under the given conditions.

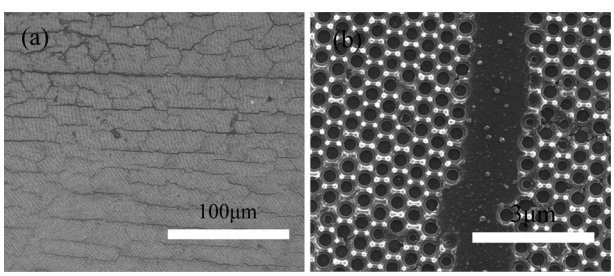

Fig. 6 SEM images of 2-D ordered architectures ($SiCl_4$: $GeCl_4$ = 1 : 1) with an area of more than 6×10^4 μm^2 (a). High resolution image shows that the cracks of the original template have been filled electrochemically, too (b).

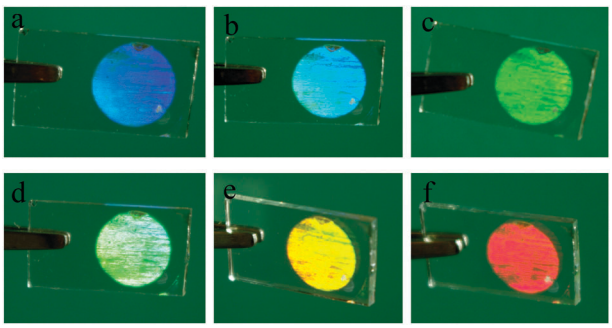

Fig. 7 Optical photographs of deposited 2-D ordered structure (PS sphere size 500 nm, $SiCl_4$: $GeCl_4$ = 1 : 1) on ITO substrate showing a color variation with changing the angle of incident white light.

Fig. 7 shows optical photographs of the 2-D ordered Si_xGe_{1-x} films electrodeposited through a PS template made of spheres with a diameter of 500 nm, showing a color change from red, yellow, light green, dark green, light blue to dark blue. The product displays a typical iridescent behavior as the incident angle between the substrate and the artificial white light is slightly changed. These measurements show without doubt that the samples have characteristics of a photonic crystal, but the *ex situ* attack by oxygen makes a quantitative analysis quite challenging, requiring optical measurements inside an argon filled glove box.

Conclusions

In this paper, we have successfully made amorphous 2-D ordered Si_xGe_{1-x} thin films with a periodic porous structure which under air unfortunately get oxidized. Electrodeposition done at an elevated temperature of 90 °C using a 3-D colloidal template delivered Si_xGe_{1-x} 2-D architectures, due to a sintering of the PS spheres and due to evaporation of $SiCl_4$ and $GeCl_4$.

The experiments prove – in principle – the successful fabrication of large dimension Si_xGe_{1-x} ($0.19 < x < 0.78$) films by adjusting the molar ratio of $SiCl_4$ and $GeCl_4$ in the electrolyte. Our approach has the potential to simplify a process for the construction of 2-D architecture and might provide an efficient and alternative way to prepare amorphous Si_xGe_{1-x} with a periodic structure for advanced applications in photovoltaics and microelectronics. For an application, however, the problem of the surface oxidation has to be solved, and annealing of the material might be one possible way out.

Acknowledgements

We thank the National Natural Science Foundation of China (No. 51010005, 90916020, 51174063), the Program for New Century Excellent Talents in University (NCET-08-0168), the Fundamental Research Funds for the Central Universities (HIT.ICRST.2010001) and Sino-German joint project (GZ550) for financial support. The support by DFG within the project EN 370/6 is also gratefully acknowledged.

Notes and references

1 X. D. Wang, E. Graugnard, J. S. King, Z. L. Wang and C. J. Summers, *Nano Lett.*, 2004, **4**, 2223.
2 T. Tatsuma, A. Ikezawa, Y. Ohko, T. Miwa, T. Matsue and A. Fujishima, *Adv. Mater.*, 2000, **12**, 643.
3 M. Kanungo and M. M. Collinson, *Chem. Commun.*, 2004, 548.
4 F. Q. Sun, W. P. Cai, Y. Li, B. Q. Cao, Y. Lei and L. D. Zhang, *Adv. Funct. Mater.*, 2004, **14**, 283.
5 B. Q. Cao, W. P. Cai, F. Q. Sun, Y. Li, Y. Lei and L. D. Zhang, *Chem. Commun.*, 2004, 1604.
6 H. W. Yan, Y. L. Yang, Z. P. Fu, B. F. Yang, L. S. Xia, S. Q. Fu and F. Q. Li, *Electrochem. Commun.*, 2005, **7**, 1117.
7 P. N. Bartlett, J. J. Baumberg, S. Coyle and M. E. Abdelsalam, *Faraday Discuss.*, 2004, **125**, 117.
8 P. Jiang, *Angew. Chem., Int. Ed.*, 2004, **43**, 5625.
9 X. H. Xia, J. P. Tu, J. Zhang, J. Y. Xiang, X. L. Wang and X. B. Zhao, *ACS Appl. Mater. Interfaces*, 2010, **2**, 186.
10 Y. Li, W. Cai and G. Duan, *Chem. Mater.*, 2008, **20**, 615.
11 R. Al-Salman, S. Zein El Abedin and F. Endres, *Phys. Chem. Chem. Phys.*, 2008, **10**, 4650.
12 R. Zhu, M. McLachlan, S. Reyntjens, F. Tariq, M. P. Ryan and D. W. McComb, *Nanoscale*, 2009, **1**, 355.
13 X. M. Deng, X. B. Liao, S. J. Han, H. Povolny and P. Agarwal, *Sol. Energy Mater. Sol. Cells*, 2000, **62**, 89.
14 D. J. Paul, *Semicond. Sci. Technol.*, 2004, **19**, R75.
15 R. Al-Salman, X. D. Meng, Y. Li, U. Kynast, M. M. Lezhnina and F. Endres, *Pure Appl. Chem.*, 2010, **82**, 1673.
16 F. Q. Sun, W. P. Cai, Y. Li, B. Q. Cao, F. Lu, G. T. Duan and L. D. Zhang, *Adv. Mater.*, 2004, **16**, 1116.
17 M. Al Zoubi, R. Al-Salman, Y. Li and F. Endres, *Z. Phys. Chem.*, 2011, **225**, 393.
18 F. Endres, N. Borisenko and S. Z. El Abedin, *Faraday Discuss.*, 2012, **154**, 221.
19 A. Oya, F. Beguin, K. Fujita and R. Benoit, *J. Mater. Sci.*, 1996, **31**, 4609.
20 X. D. Meng, R. Al-Salman, J. P. Zhao, N. Borissenko, Y. Li and F. Endres, *Angew. Chem., Int. Ed.*, 2009, **48**, 2073.
21 G. Subramania, R. Biswas, K. Constant, M. M. Sigalas and K. M. Ho, *Phys. Rev. B: Condens. Matter*, 2001, **63**, 235111.
22 Y. An, S. J. Skinner and D. W. McComb, *J. Mater. Chem.*, 2010, **20**, 248.
23 Y. Li, C. C. Li, S. O. Cho, G. T. Duan and W. P. Cai, *Langmuir*, 2007, **23**, 9802.
24 N. Sapoletova, T. Makarevich, K. Napolskii, E. Mishina, A. Eliseev, A. van Etteger, T. Rasing and G. Tsirlina, *Phys. Chem. Chem. Phys.*, 2010, **12**, 15414.

